Radio Science, Volume 28, Number 1, Pages 49–61, January–February 1993

A first-principle derivation of the high-latitude total electron content distribution

D. J. Crain, J. J. Sojka, AND R. W. Schunk

Center for Atmospheric and Space Sciences, Utah State University, Logan, Utah

P. H. Doherty

Institute for Space Research, Boston College, Newton, Massachusetts

J. A. Klobuchar

Space Physics Division, Geophysics Directorate, Phillips Laboratory, Hanscom Air Force Base, Massachusetts

(Received March 3, 1992; revised August 3, 1992; accepted August 3, 1992.)

Calculation of the high-latitude distribution of the vertical total electron content (TEC) is possible using a three-dimensional, time-dependent ionospheric model. Global and local comparisons may be made with observations of TEC. We compare the local diurnal variation of TEC calculated by the model with observations of TEC at Goose Bay, Labrador and Hamilton, Massachusetts. Data from the period of March 1–11, 1989, and monthly averaged data for solar maximum and solar minimum periods are examined. We extend the model to predict diurnal variations of TEC in the polar cap and compare these results with the observed TEC at Thule, Greenland, during an 8-day campaign from January 28 through February 4, 1984. We propose a possible explanation for the large variability observed. We show that the "equivalent vertical content" TEC is very sensitive to horizontal F layer electron density gradients and that such "equivalent vertical" TECs may vary significantly from the true vertical TEC of the ionosphere. By incorporating these results, we calculate the vertical TEC distribution of the high-latitude ionosphere for a wide range of solar activity, seasons, and Kp variation represented by a recently completed Utah State University time-dependent ionospheric model data base. Finally, we discuss the possible uses of TEC as a diagnostic tool for testing ionospheric models.

1. INTRODUCTION

Previous models of the global total electron content (TEC) distribution have generally relied on empirically derived ionospheric models of f_oF_2 and the topside slab thickness to calculate TEC [*Llewellyn and Bent*, 1973; *Ching and Chiu*, 1973; *Chiu*, 1975; *Kohnlein*, 1978; *Rawer*, 1981]. A significant problem with such models at high latitudes is the considerable degree of structure induced by auroral and magnetospheric convection processes and the lack of coverage of ionosonde and TEC receivers at high latitudes. In lieu of an extensive geographic array of digisondes and TEC receivers required to construct an adequate empirical model of the high-latitude TEC distribution, we have attempted to determine the TEC distribution over the entire polar cap by using a first-principle model of the high-latitude ionosphere. The Utah State University (USU) time-dependent ionospheric model (TDIM) developed by Schunk and coworkers is used for this study [*Schunk et al.*, 1986; *Sojka and Schunk*, 1985]. Such a model naturally incorporates the effects of high-latitude convection and auroral precipitation to self-consistently solve the continuity, energy, and momentum equations for the ionospheric plasma. These processes produce considerable structure in the real high-latitude ionosphere. This structure is observed in TEC data and is reproduced by realistic models. The TEC derived from the model is compared with the Air Force Geophysics Laboratory (U.S. Air Force Air Weather Service) data sets of TEC determined by Faraday rotation of a radio carrier transmitted from a geosynchronous satellite and received at Goose Bay, Labrador, and Hamilton,

Copyright 1993 by the American Geophysical Union.

Paper number 92RS01928.
0048-6604/93/92RS-01928$08.00.

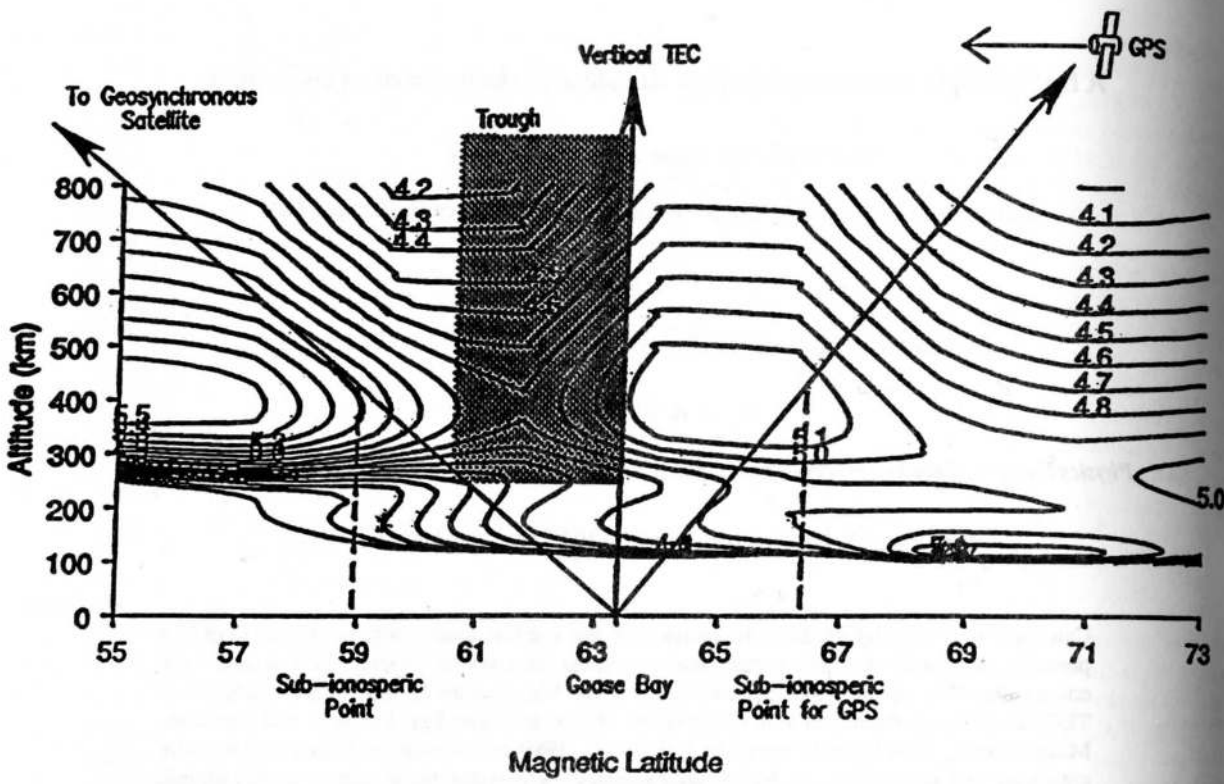

Fig. 1. Meridional slice of the ionospheric electron density at 0100 UT, 2100 MLT for winter solar maximum and $Kp = 3.5$. The geographic location of Goose Bay, Labrador, is shown, along with the geometry of straight-line ray paths used to determine TEC from geosychronous and polar orbiting satellite beacons. The subionospheric point for each ray is also shown.

Massachusetts. Monthly averaged and daily TECs are compared with the model results.

Figure 1 is a schematic of some possible satellite/receiver geometries that may exist at Goose Bay. This contour plot is a meridional slice of the ionospheric electron density at 0100 UT, 2100 MLT for winter solar maximum, $Kp = 3.5$, and $B_y > 0$. Shown on the plot is the approximate ray path to the geosynchronous point from the location of Goose Bay. This path defines the sub ionospheric point where the ray intersects 420 km altitude. The TEC along this ray path approximates the "columnar content" at this sub ionospheric point for a ray path intersecting the ionosphere at 420 km [*Mendillo and Klobuchar*, 1975]. Also shown are some of the actual large-scale plasma structures present in the high-latitude evening ionosphere, such as the trough. Most of the time the trough is missed by the ray path, but if convection changes or magnetic activity increases, the trough may move through the ray path, causing a corresponding decrease in the observed TEC. Note that a high-inclination spacecraft such as GPS would allow the spatial structure of the trough to be examined by observation of TEC as the ray path moves through the trough. Even though a GPS satellite has a fairly slow ground track (due to its 10,000 km orbital altitude), a statistical examination of many such crossings of the trough region may help elucidate the seasonal, solar cycle, spatial, and temporal characteristics of the trough. If a TEC transmitter is available on a lower-altitude spacecraft with a high-inclination orbit then a more instantaneous picture of the trough region may be constructed as the satellite transmitter-ground receiver ray path rapidly transects the region. Several such sites situated throughout the high-latitude region could provide enough coverage that the large-scale structuring, for example, of the polar ionosphere could be reasonably monitored. This would provide excellent validation and relevant inputs and constraints (N_mF_2, N_{max}, TEC) for realistic high-latitude ionospheric models.

The model is used to extend predictions of the diurnally varying TEC to higher geomagnetic latitudes and to produce contour maps of TEC for the entire polar region for various input parameters. This enables us to predict the spatial variation of TEC observed by a fixed receiver and a high-inclination satellite, such as the Global Positioning System (GPS), for various transmitter receiver geometries in the polar region.

Besides the practical aspects of TEC prediction, the use of TEC as a diagnostic tool for first-principle models is examined. An ionospheric model's ability to reproduce the actual ionosphere usually is indicated by comparing the model output of h_mF2, N_mF2, and perhaps N_e at some particular altitude (such as one which intersects a satellite's orbit) with an observation of the same parameters in the real ionosphere. If an incoherent scatter radar is available, many more data are available to compare with the output of a particular model. A measurement of TEC contains information about the shape (or thickness) of the upper F region. This shape is dependent upon density, temperature, transport, and other processes that are not explicitly evident in an examination of h_mF2, and N_mF2. Therefore the use of TEC in conjunction with other available parameters can improve the ability of a model to reproduce the actual ionosphere and lead to insights as to the actual processes that influence TEC and the F region plasma.

2. OBSERVATIONAL DATA

The ionospheric TEC data used in this study have been calculated from measurements of Faraday polarization rotation using VHF signals transmitted from geostationary satellites. These measurements of Faraday polarization produce slant TEC (TEC along a line of sight). These slant values have been converted to equivalent vertical TEC at the subionospheric point, defined as where the ray path intersects the mean ionospheric height. The U.S. Air Force Air Weather Service operates a number of stations that make continuous measurements of TEC using this technique [*von Flutow*, 1978]. TEC data have been obtained in this manner for at least one complete solar cycle from several stations. Table 1 lists the stations, time periods, and subionospheric coordinates of the data referenced in this study.

3. MODEL DESCRIPTION

The ionospheric model used in this study is a data set constructed from a large set of runs of the USU/TDIM. The TDIM is a first-principle model which solves the continuity, momentum, and energy equations for O^+, O_2^+, NO^+, N_2^+, N^+, and He^+ along convecting flux tubes between 88 and 800 km. The model has been described extensively by *Schunk et al.* [1986] and compared with the observations by *Sojka and Schunk* [1985]. For the purposes of global studies such as this, the model has been run in such a way as to construct a snapshot of the high-latitude ionosphere at fixed UTs for a particular condition of solar activity, Kp, interplanetary magnetic field (IMF) orientation, and season. Auroral precipitation and magnetospheric/ionospheric convection are based on a Hardy statistical precipitation [*Hardy et al.*, 1987] oval and Heppner-Maynard [*Heppner and Maynard*, 1987] convection for southward IMF.

TABLE 1. TEC Observational Data Base

Station	Time Period	Sub-Ionospheric Latitude	Sub-Ionospheric Longitude
Goose Bay, Laboratory	1981	47° N	298° E
	1986	47° N	285° E
	March 1989	47° N	285° E
Hamilton, Mass.	1981	39° N	290° E
	1986	39° N	282° E
	March 1989	39° N	282° E

The environmental parameters used in the model to construct these data sets are $F10.7$ flux (maximum (210), medium (130), and minimum (70)), season (winter, summer, and equinox), IMF B_y orientation ($B_y < 0$, $B_y > 0$), and Kp index (6, 3.5, and 1). Variation of all the environmental parameters yields a data set representing 54 combinations of these parameters for the northern hemisphere.

Each of these 54 data sets consists of an array of ($20 \times 24 \times 12 \times 37 \times 3$) components representing the altitude distribution of O^+, NO^+, and O_2^+ between 100 and 800 km (37 steps) binned by UT (12 bins), magnetic latitude (20 bins, 50° to 90° in 2° steps) and MLT (24 bins in 1-hour steps). From this array we can compute the TEC contribution due to the presence of these three ions along an arbitrary straight-line path through the ionosphere. In all cases presented here, TEC computed by the model is either a true vertical content TEC or an equivalent vertical content TEC derived from a straight-line ray path between transmitter and receiver.

4. STATION COMPARISON

In order to establish the ability of the model to represent the observed diurnal variation of the high-latitude TEC adequately, we compare the results of the model with the observed TEC variation at two locations where TEC is regularly determined. Figure 2 shows the monthly averaged TEC for January of 1986 and 1981 observed at Goose Bay, Labrador, and Hamilton, Massachusetts. These data are compared to the model outputs for winter solstice, solar maximum and minimum, $Kp = 3.5$, and $B_y > 0$. Figures 2*a* and 2*b* compare observations and model results at Goose Bay for winter solar maximum and minimum. The general agreement is good, but the predicted TEC consistently is lower than the observed TEC. Figures 2*c* and 2*d* show a similar comparison between the observed TEC at Hamilton and the model TEC for the same conditions as in Figures 2*a* and 2*b*. The model generally trends with the observed TEC during the day but is significantly lower than the observed TEC at night.

Figure 3 shows the observed variation of TEC for the same stations, but for June data, compared to the model prediction for summer solar maximum and minimum. There is good agreement at both stations for solar maximum, but the model predicts TECs considerably lower (a factor of about 2–3) than

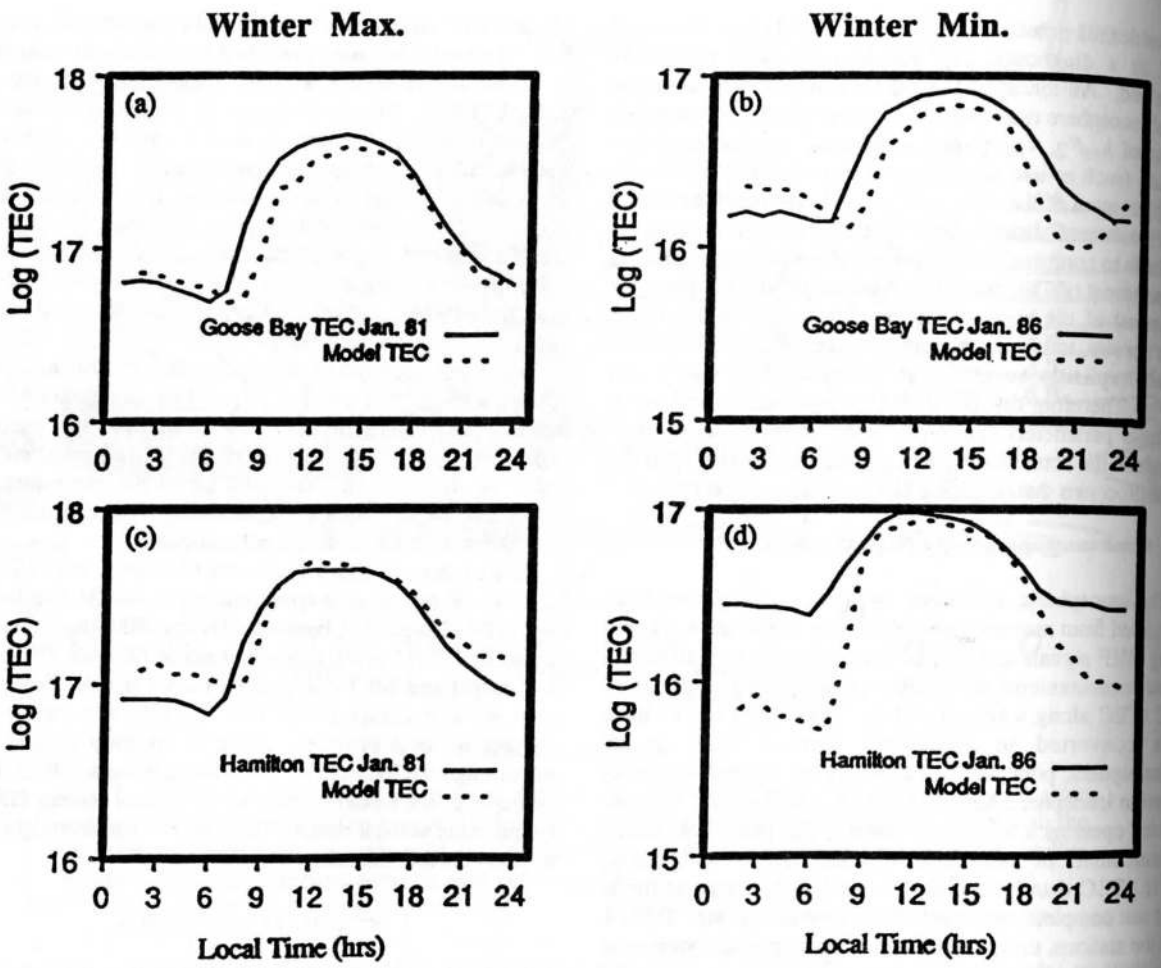

Fig. 2. Comparison of winter solar maximum and minimum TEC observed at Goose Bay, Labrador, and Hamilton, Massachusetts, and the predicted TEC derived from the TDIM model.

the observed values at both stations for solar minimum. The largest winter discrepancy occurred at nighttime during solar minimum, where the model TEC is a factor of 4 lower than the observed Hamilton TEC. This discrepancy may be produced by an enhanced contribution of TEC by plasmaspheric H^+. This is most pronounced during solar minimum, when the H^+/O^+ transition height falls to ~500 km. Therefore during solar minimum the contribution of H^+ to TEC may not be negligible. In summer the same nighttime situation arises for solar minimum at Hamilton. However, in addition, the daytime densities at both stations for solar minimum are almost a factor of 2 lower in the model. The source of this TEC difference is less obvious and will be discussed later.

The effect of the trough with changing magnetic latitude at Goose Bay longitudes is illustrated in Figure 4, which shows the model vertical TEC at 57°, 59°, 61°, and 63° magnetic latitude for Goose Bay longitudes. The trough effect is seen at different local times at each latitude. In fact, for the 6° latitude range spanned by these model results, the trough minimum has moved 4 hours in local time. This is consistent with the results of *Whalen* [1989], which examined the latitudinal and longitudinal location of the *F* region trough at high latitudes. Usually, the subionospheric point for the ray path between a geostationary transmitter and the Goose Bay receiver lies equatorward of the trough region, as shown in Figure 1. Any change in the overall convection pattern or magnetic activity that moves the trough region equatorward may produce significant changes in the TEC observed at Goose Bay as the trough moves into and out of the ray path used to determine TEC.

Some of these features predicted by the model, while not present in the monthly averaged data, may be present in the day-to-day variation of the observed TEC. The effect of the

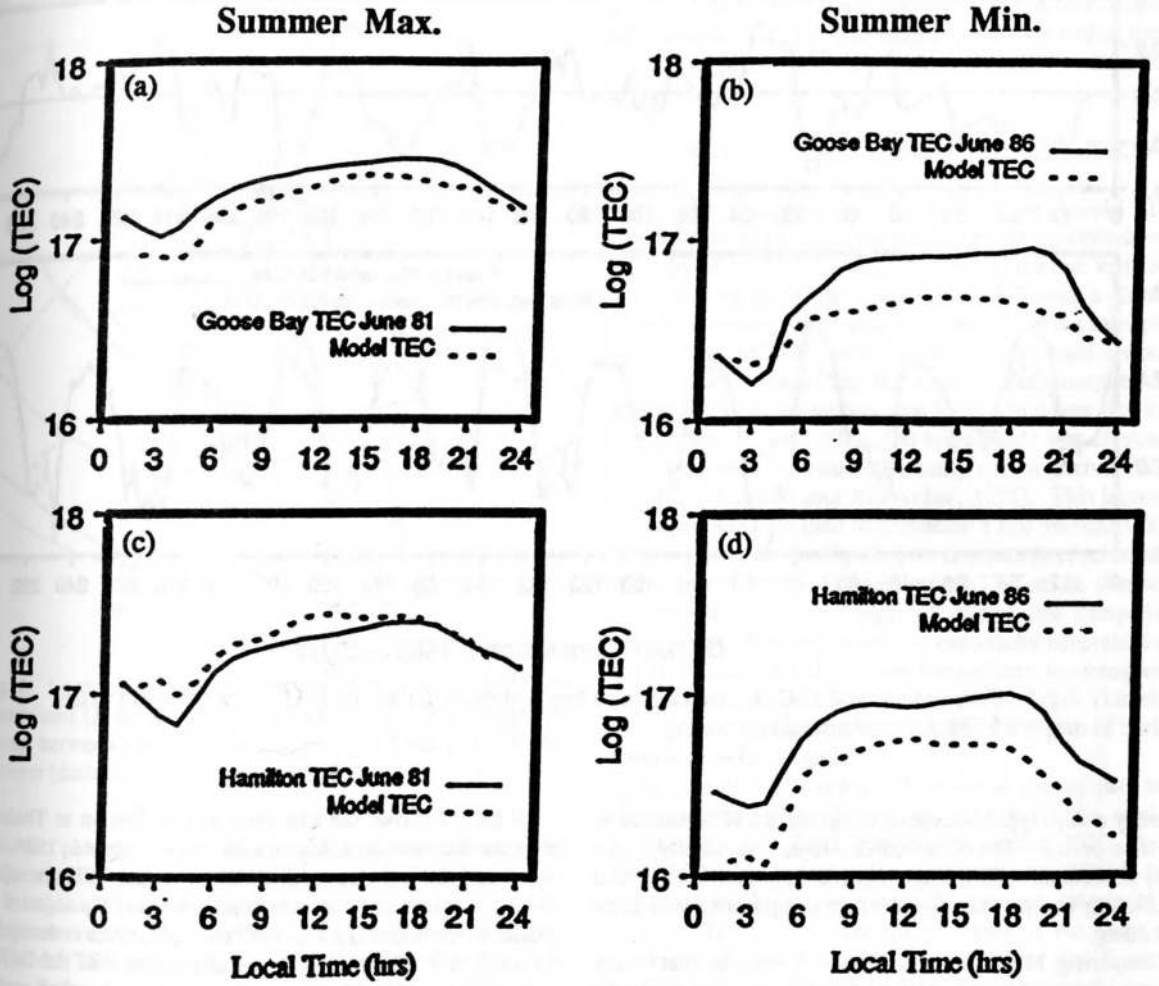

Fig. 3. Comparison of summer solar maximum and minimum TEC observed at Goose Bay, Labrador, and Hamilton, Massachusetts, and the predicted TEC.

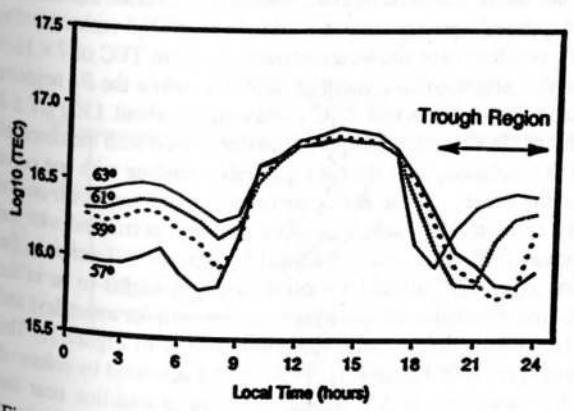

Fig. 4. Comparison of the vertical TEC derived from the TDIM model for different magnetic latitudes shown the effect of the trough for a particular Kp and IMF orientation.

trough in the TEC observed at Goose Bay is evident when the diurnal variation of TEC is examined over several successive days for a range of Kp values and IMF orientations. Such a range of conditions existed over several days in March 1989. An examination of eleven successive days demonstrates the range in variability in TEC observed at Goose Bay. Figure 5 (lower panel) compares the TEC observed March 1–10, 1989, to model TEC predictions for the average condition for this period. The top panel of Figure 5 represents the variation of the observed TEC with respect to the modeled TEC as a logarithmic difference in TEC. The model conditions used are for equinox, solar maximum, $B_y < 0$, and $Kp = 3.5$. From the upper panel in Figure 5, one sees that the model TEC usually is higher at night and lower during the day, indicating that the modeled TEC is lower during the day and higher at night. The general agreement is good, though the model does not show the same degree of variability as the observed TEC. It is

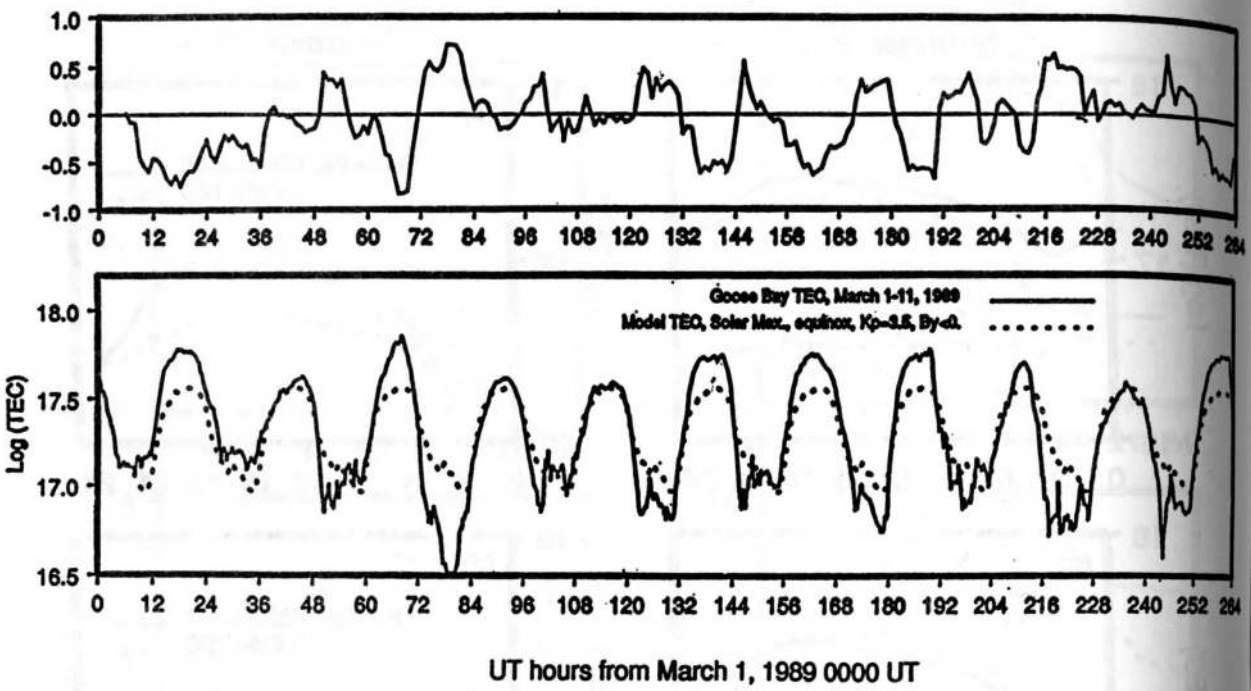

Fig. 5. Daily variation of TEC observed at Goose Bay, Labrador, for March 1–11, 1989 compared to the predicted TEC for similar conditions.

probably a fair representation of the average TEC observed in this time period. The observed day-to-day variability is not easily associated with a single *Kp* index, which implies that specific-day comparisons and average comparisons tend to be misleading.

Comparing Figure 4 with Figure 5 reveals that many features observed in the data in the evening sector can be reproduced by the model by varying the latitude of the subionospheric point. This is representative of the range of variation in TEC observed in the March period. This is equivalent to a large-scale movement and/or variation of the trough region with respect to the receiver at Goose Bay.

5. THULE, GREENLAND PREDICTIONS

In order to examine the predictions of the model in the polar cap in more detail, we compare the model results with a particular TEC observation campaign, which occurred in the time period of January 28 through February 4, 1984. This campaign is described in detail by *Klobuchar et al.* [1985]. It represented the first measurements of TEC made from a polar cap station using the Global Positioning System (GPS) satellites. Figure 6 shows the spatial region around Thule, Greenland, where GPS TEC measurements were made. The dashed lines represent the ground track of the subionospheric point for TEC observations during the study. The letters A-E denote locations where TEC was calculated by the model.

Figure 7 shows the observed TEC variation at Thule for two consecutive days, January 31 and February 1, 1984. The solid and dashed lines represent the model TEC for winter, solar minimum, *Kp*-medium conditions and B_y negative and positive, respectively. The TEC for both curves is determined at point A in Figure 6. The hourly average of the IMF B_y component is mostly positive throughout this period, and B_z is southward within the regions indicated and northward elsewhere. IMF data were obtained from the NSSDC OMNI data base. From the model results it is evident that the IMF may have a strong control of the diurnal TEC variation. The B_y positive case shows a relatively uniform TEC of 7×10^{16} with a slight enhancement at 0800 LT, while the B_y negative case shows a marked TEC enhancement about 1300 LT ± 3 hours. Both curves compare reasonably well with the observed TEC variation, with the data generally trending with one curve or the other. While the observations trend well with one or the other model curves, they are not well correlated with the actual IMF variation. The most significant difference in the observed TEC diurnal variation at Thule seems to be in the degree of enhanced TEC structure observed for some days and absent for others. This variation is seen in Figure 7. The noon period of January 31, 1984, is characterized by enhanced TEC structure, which seems to follow a baseline near the model curve. The noon period of the following day does not have the same degree of enhanced TEC structure. These enhanced TEC structures have been interpreted as signatures of

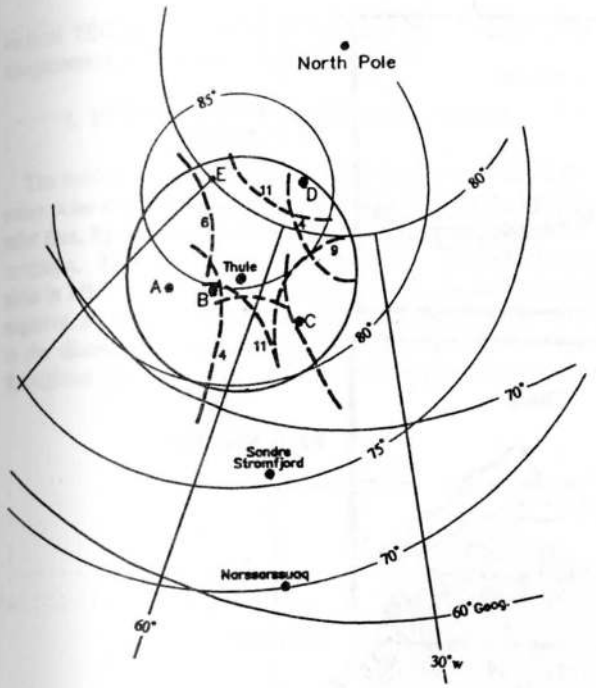

Fig. 6. Location of subionospheric points in which TEC was determined (A-E) and the ground track of the subionospheric points between the GPS satellite and the Thule, Greenland, receiver (dashed lines) [*Klobuchar et al.*, 1985].

plasma "patches" [*Klobuchar et al.*, 1985] and are most frequently observed when the IMF is southward.

In addition to the modeled variation due to the B_y component of the IMF, there is significant spatial variation of the model TEC around Thule, which is shown in Figure 8. Figure 8 also shows the diurnal variation of TEC for different azimuths and elevations around Thule and for different B_y orientations. These azimuths and elevations correspond to the subionospheric points denoted in Figure 6. There is also a considerable Kp variation, not shown here, which may vary TEC by a factor of 2 at a particular subionospheric point. The effect of the IMF, Kp, and spatial variability within the polar cap can account for much of the variability in the observed TEC.

6. SLANT TEC VERSUS VERTICAL TEC

Another important feature that we would like to demonstrate is the difference between an equivalent vertical TEC derived from a slanted ray path and the true vertical TEC derived from the model. When the TEC from a slanted ray path is computed, any horizontal structure in the ionosphere is included in the TEC. In this study we computed not only the TEC from a slanted ray but also the subionospheric point along the ray at the latitude and longitude where the ray path intersected 420 km. (The 420 km altitude was chosen to be consistent with the method normally used to derive TEC from satellite [*Mendillo and Klobuchar*, 1975]. This latitude and longitude was then used to determine a true vertical TEC from the model output. In Figure 9 we compare the equivalent TEC from a slant path to the true vertical TEC at the slanted ray's subionospheric point. Figure 9 shows this comparison at Goose Bay. The two curves are essentially equivalent during the day, where no significant ionospheric inhomogeneity is present, but are significantly different at night. This effect is most pronounced during winter, when the degree of horizontal variability is the greatest.

In general, the lower the elevation of the ray path and the more structured the ionosphere, the more the equivalent vertical TEC will differ from the true vertical TEC. But even for a highly structured polar cap ionosphere, TEC is heavily weighted by the region where the ray path intersects the F region. Therefore horizontal gradients of the order of the thickness of the F layer will have the most significant effect on TEC. The scale size of such gradients would be of the order of 200 km or so and is at the latitudinal resolution of this study. Therefore the difference between true vertical TEC and equivalent TEC may be underestimated here. Nonetheless, we see that at the resolution of this study the equivalent

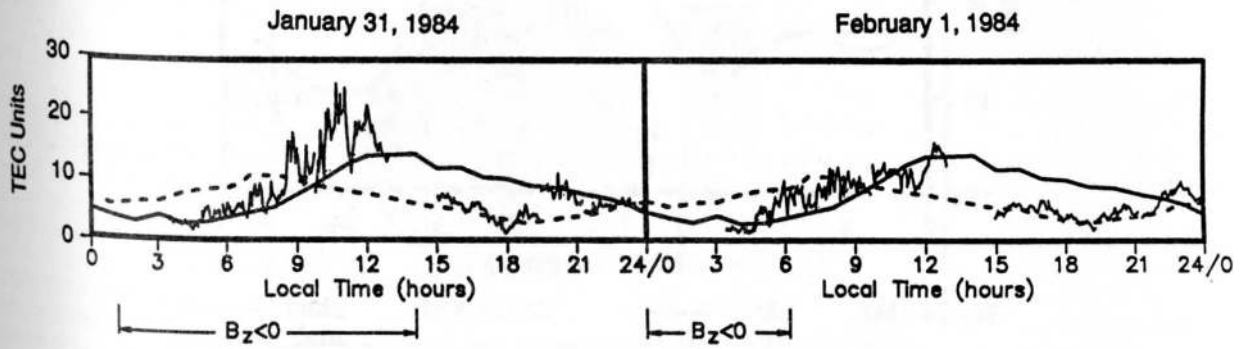

Fig. 7. Observed TEC variation for January 31 and February 1, 1984, at Thule, Greenland, compared to modeled TEC for $B_y < 0$ and $B_y > 0$, winter solar medium conditions.

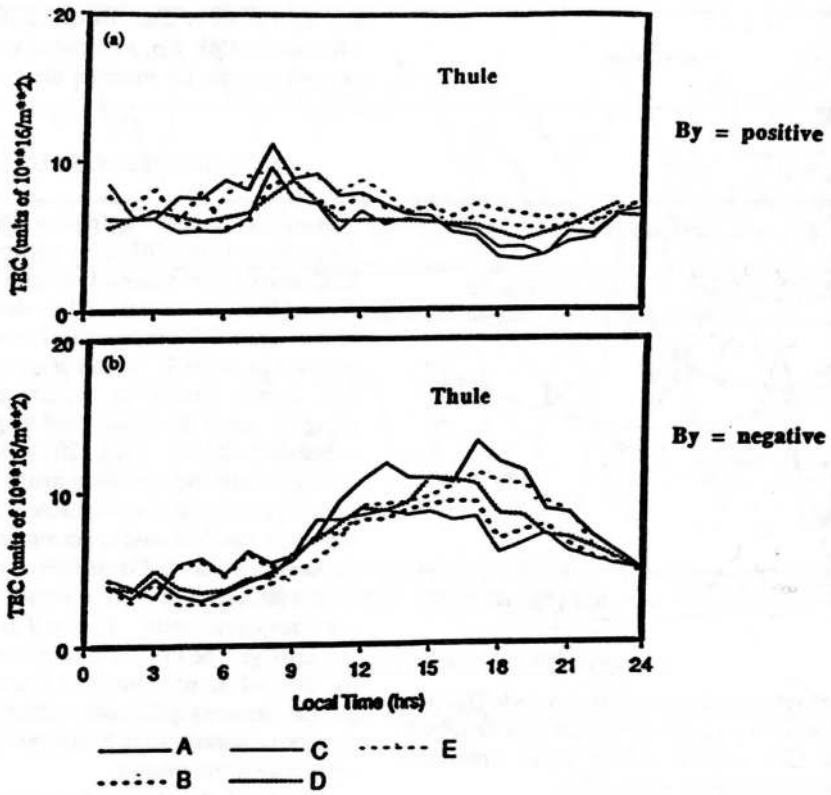

Fig. 8. Modeled TEC showing spatial variations and variation due to IMF B_y orientation for various subionospheric points surrounding Thule, Greenland, corresponding to the January 28 – February 4, 1984, observation campaign.

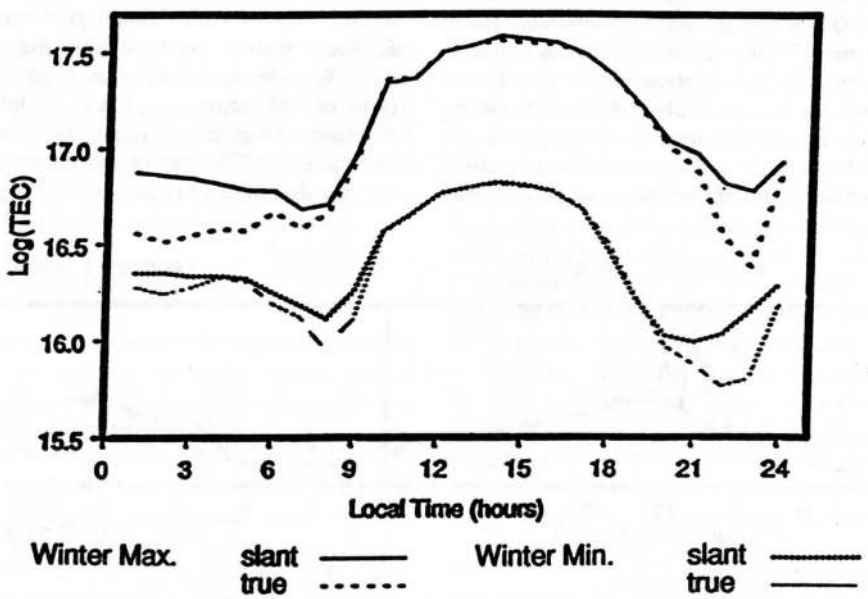

Fig. 9. Comparison of derived columnar content from the slant ray path and true vertical TEC derived at the subionospheric point for Goose Bay, Labrador.

vertical TEC and true vertical TEC can show considerable disagreement, with factors of 2 being possible.

7. HIGH-LATITUDE TEC DISTRIBUTIONS

The model TEC prediction can be extended to include the entire polar cap to provide the vertical TEC at a particular UT, solar flux, Kp and season for all MLTs and latitudes above 50° invariant. Figure 10*a* and 10*b* shows such a series of dial plots in MLT coordinates for solar maximum, B_y positive and negative, B_z southward, and $Kp = 3.5$. The features observed in the diurnal variation at individual stations can be seen throughout the polar dial. Winter TEC distributions show much more structure and more pronounced convection features than do the TEC distributions for summer and equinox. Winter and equinox TECs always show evidence of the mid-latitude trough, but the TEC signature of the trough is almost indistinguishable from the rest of the polar cap in summer.

To a lesser degree, there are UT effects in the high-latitude TEC distribution, which could be observed by TEC observation stations at similar magnetic latitudes but different longitudes. Figure 11 illustrates the type of UT variation that can be expected for solar medium conditions, winter, $Kp = 3.5$, and $B_y > 0$.

These polar contour plots illustrate the importance of a realistic ionosphere model that includes convection effects.

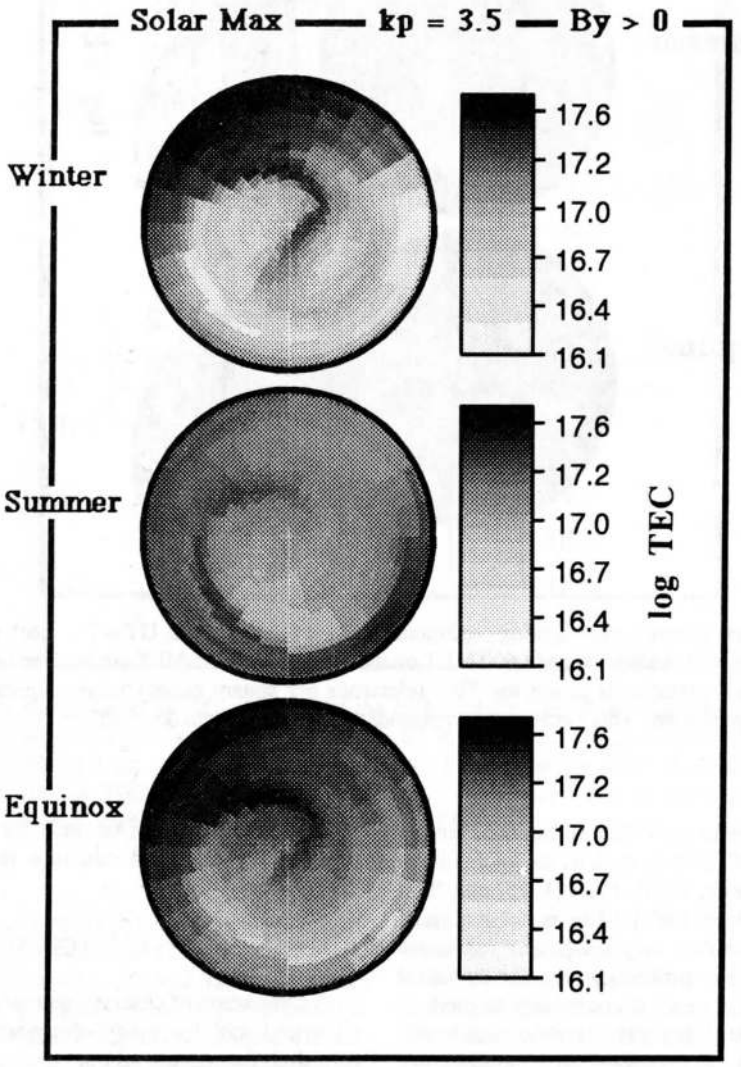

Fig. 10*a*. Gray scale polar dial plots of the TEC distribution for solar maximum conditions, $Kp = 3.5$. Winter, summer, and equinox conditions for $B_y > 0$, and $B_z < 0$, UT = 21.

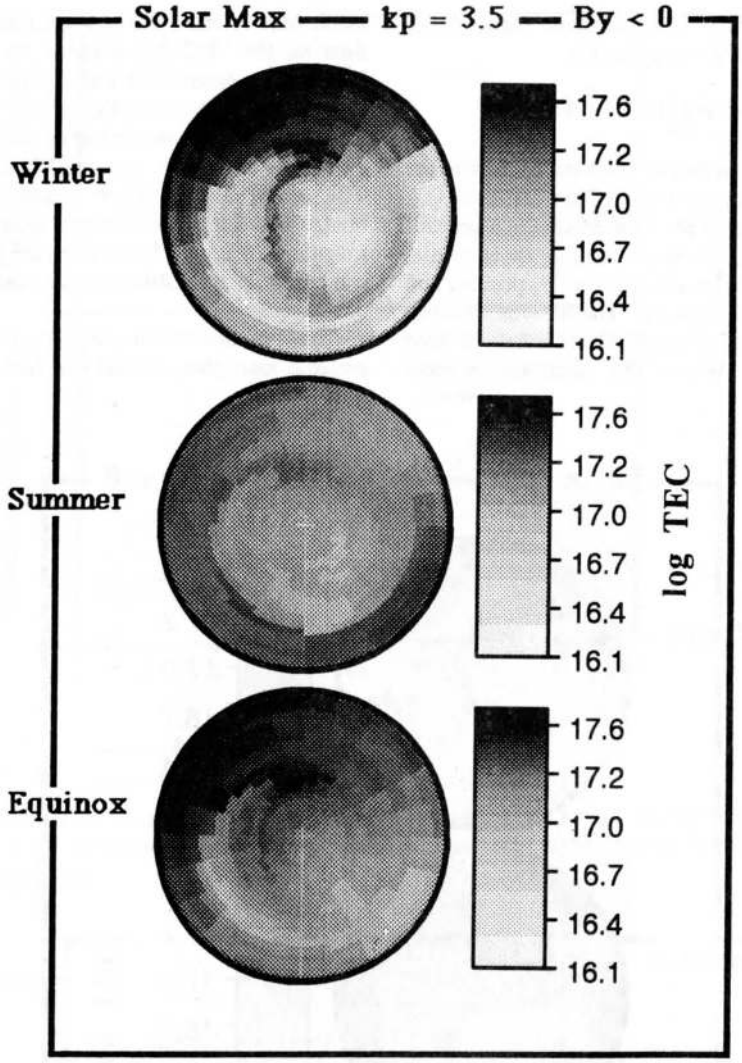

Fig. 10*b*. Winter, summer, and equinox conditions for $B_y < 0$, and $B_z < 0$, UT = 21. Each polar dial has magnetic midnight at the bottom and 0600 MLT on the right edge of the MLT circle. The bar scale at the left of each dial corresponds to the log TEC (electrons per square meter) values represented by the corresponding gray scale. This circle also corresponds to a magnetic latitude of 50°.

The high degree of structure in the TEC distribution is simply not present in some "global" models, such as the international reference ionosphere [*Rawer*, 1981], *Chiu* [1975] and Bent models [*Llewellyn and Bent*, 1973]. This is not a fault of these particular models, for they very adequately reproduce TECs at lower latitudes. The problem is that for empirical models, there is simply not enough data coverage to produce realistic TEC profiles at high latitudes. In other words, the high-latitude ionosphere is too dynamic to be statistically modeled with data sets that use single satellite passes spread over many years. In addition, the effects of convection and auroral processes must be included in some realistic way to produce the observed structure in the high-latitude TEC distribution.

8. DISCUSSION

A comparison of observed and model TEC values can be an important tool for model diagnostics. TEC observations reveal information about the structure, temperature, composition, and density of the ionospheric plasma that are not available from single point measurements of ionosphere

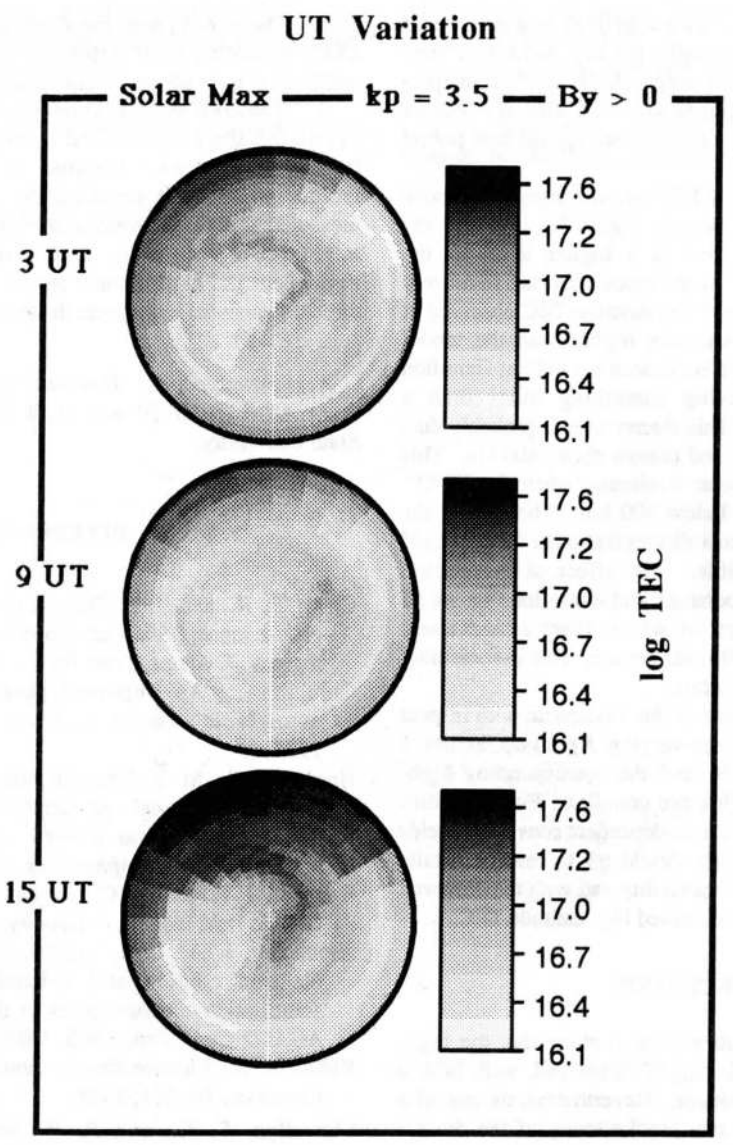

Fig. 11. Gray scale plot of the UT variation of the high-latitude TEC distribution for solar maximum conditions, winter, $Kp = 3.5$, and $B_z < 0$, and $B_y > 0$. Each polar dial has magnetic midnight at the bottom and 0600 MLT on the right edge of the MLT circle. The bar scale at the left of each dial corresponds to the log TEC (electrons per square meter) values represented by the corresponding gray scale. This circle also corresponds to a magnetic latitude of 50°.

parameters such as h_mF_2 or N_mF_2. A good agreement between observations and the results of a first-principle model with TEC, along with observed h_mF_2 and N_mF_2, increases confidence in the physical processes and assumptions included in the model. When the observed TEC does not agree with the model prediction, but h_mF_2 and N_mF_2 are in agreement, then this discrepancy is revealing something important that may need consideration. In the case of Figures 2 and 3, the model consistently underestimates, on average, the observed TEC. What does this tell us?

For the model runs used in this study, plasma density was determined only up to 800 km. The method by which TEC is determined at Goose Bay and Hamilton gives the TEC up to 2000 km. Thus we are systematically neglecting a region that makes a consistent, though small, contribution to the total TEC. In addition, the model does not calculate the H^+

distribution or the H^+ flux. This may lead to a significant underestimate of TEC, especially for ray paths that pass through the plasmasphere or when the H^+/O^+ transition altitude is low. This corresponds well with what is observed at Hamilton, Massachusetts, during the solar minimum period in Figures 2*d* and 3*d*.

This component of the total TEC due to composition above 800 km and H^+ is most evident in Figure 2*d*, in which the nighttime TEC is maintained at a higher level in the observation than is predicted by the model. During summer, a similar effect is observed, with the daytime TEC observed at solar minimum being significantly higher than the model prediction. In this case the effect is seen not only at Hamilton but at Goose Bay, implying something other than a plasmaspheric mechanism. This discrepancy is probably due, in part, to the neglect of H^+ and plasma above 800 km. This is important especially at solar minimum, when the H^+/O^+ transition altitude may fall below 500 km. The size of the discrepancy at solar minimum indicates that other factors could be at least partly responsible. The effect of the neutral atmosphere, exospheric temperature, and ionization flux are all important input parameters in which there is sufficient uncertainty to contribute to this difference. This is something that should be studied in the future.

The actual time dependence of the ionosphere with respect to such parameters as a time-varying *Kp* index and/or a dynamic and changing IMF (and the corresponding high-latitude convection) is much more complex. Future studies that incorporate more realistic time-dependent convection fields and high-latitude precipitation should try to resolve results with day-to-day mid-latitude variability and with the observed short-period variations of the observed high-latitude TEC.

9. CONCLUSION

In this paper we have attempted to show that the high-latitude TEC distribution is highly structured, with both a seasonal and an IMF dependence. Nevertheless, the use of a realistic ionosphere model can predict many of the diurnal features observed in TEC at locations such as Goose Bay, Labrador, and Thule, Greenland.

We summarize with the following observations:

1. Realistic ionospheric models that include convection are needed to adequately predict high-latitude TEC distribution.

2. Spatial structure must be considered when using slant path TECs to construct vertical TEC distributions. Vertical equivalent TEC and true vertical TEC are not always the same thing.

3. Much of the daily variability in TEC observed at very high latitudes such as at Thule, Greenland, can be, at least partially, attributed to the spatial variation and IMF dependence of TEC at high latitudes.

4. Because much of the high-latitude structure in TEC is due to convection effects, models that neglect convection may not be adequate to predict high-latitude TEC.

5. The plasma near the *F* peak contributes the most to TEC, but during solar minimum, the contribution from H^+ and from plasma above 800 km may be significant.

6. The GPS satellite provides an excellent platform for examining the temporal and spatial structure of the high-latitude ionosphere. Because of its slow-moving high-inclination orbit, it provides the potential to make TEC measurements that geostationary beacons cannot provide. It might prove fruitful to have a chain of TEC receivers throughout the high-latitude region to cheaply map the real three-dimensional ionosphere distribution.

Acknowledgments. This research was supported by NSF grant ATM-89-13230 and grant AFOSR-90-0026 to Utah State University.

REFERENCES

Ching, B. K., and Y. T. Chiu, A phenomenological model of global ionospheric electron density in the *E*, F_1 and F_2 regions, *J. Atmos. Terr. Phys., 35*, 1615, 1973.

Chiu, Y. T., An improved phenomenological model of ionospheric density, *J. Atmos. Terr. Phys., 37*, 1563, 1975.

Hardy, D. A., M. S. Gussenhoven, R. Raistrick, and W. J. McNeil, Statistical and functional representations of the pattern of auroral energy flux, number flux, and conductivity, *J. Geophys. Res., 92*, 12,275, 1987.

Heppner, J. P., and N. C. Maynard, Empirical high-latitude electric field models, *J. Geophys. Res., 92*, 4467, 1987.

Klobuchar, J. A., G. J. Bishop, and P. H. Doherty, Total electron content and L-band amplitude and phase scintillation measurements in the polar cap ionosphere, *AGARD Conf. Proc.*, 382, 1985.

Kohnlein, W., Electron density models of the ionosphere, *Rev. Geophys., 16*, 341, 1978.

Llewellyn, S. K., and R. B. Bent, Documentation and description of the Bent ionospheric model, Rep. AFCRL-TR-73-0657, AD 772–733, 1973.

Mendillo, M., and J. A. Klobuchar, Investigations of the ionospheric *F* region using multi-station total electron content observations, *J. Geophys. Res., 80*, 643, 1975.

Rawer, K., International reference ionosphere-IRI 79, *NOAA Rep., UAG-82*, U.S. Dep. of Commerce, Washington, D. C., 1981.

Schunk, R. W., J. J. Sojka, and M. D. Bowline, Theoretical study of the electron temperature in the high latitude ionosphere for solar maximum and winter conditions, *J. Geophys. Res., 91*, 12,041, 1986.

Sojka, J. J., and R. W. Schunk, A theoretical study of the global *F* region for June solstice, solar maximum, and low magnetic activity, *J. Geophys. Res., 90*, 5285, 1985.

von Flutow, C. S., Ionospheric forecasting at Air Force

Global Weather Central, in *Effect of the Ionosphere on Space and Terrestrial Systems*, U.S. Government Printing Office, Washington, D. C., 1978.

Whalen, J. A., The daytime *F* layer trough and its relation to ionospheric-magnetospheric convection, *J. Geophys. Res.*, *94*, 17,169, 1989.

D. J. Crain, R. W. Schunk, and J. J. Sojka Center for Atmospheric and Space Sciences, Utah State University, Logan, UT 84322-4405.

P. H. Doherty, Institute for Space Research, Boston College, Newton, MA 01259.

J. A. Klobuchar, Space Physics Division, Geophysics Directorate, Phillips Laboratory, Hanscom Air Force Base, MA 01731.